The Illumination of Natural Fractures and Faults of the Muskwa Shale Play in Northeastern British Columbia: A Case Study*

Jane Ling[1] and William Barker[2]

Search and Discovery Article #41507 (2014)
Posted December 29, 2014

*Adapted from extended abstract prepared in conjunction with oral presentation at CSPG/CSEG/CWLS GeoConvention 2013, (Integration: Geoscience engineering Partnership) Calgary TELUS Convention Centre & ERCB Core Research Centre, Calgary, AB, Canada, 6-12 May 2013, AAPG/CSPG©2014

[1]MicroSeismic Canada ULC, Calgary AB Canada (jling@microseismic.com)
[2]MicroSeismic Inc., Houston, Texas

Summary

In this case study we discuss the natural fracture and faulting characteristics of the Muskwa Shale play in Northeastern British Columbia. The Muskwa is an ideal area for studying the acoustic effects of hydraulic fracture stimulation as these shales are known to be generally very brittle, expressing interesting characteristics, such as lengthy linear fractures. The microseismic data for this study was recorded by a surface array during the hydraulic fracturing for 9 horizontal wells, 8 of them located within the Muskwa Formation. Two different completion techniques were used affecting how the rock fractured—(1) perforation and plug and (2) ball and sliding sleeve. The major trend seen in the data is a 70º fracture azimuth. These linear fractures are a phenomenon that can be explained by geologic analysis of the area, natural stresses in the rock, and the type of completion technique used. Specific wells in this pad are discussed, illustrating different geologic characteristics, stimulated fracture geometry, and the performance of the completion, including focal mechanism and b-values analysis.

Introduction

The microseismic data for this study was recorded during the hydraulic fracturing of 9 horizontal wells, 8 of them (Figure 1) located within the Muskwa Formation in Northeastern British Columbia. The general trends in the treatments, as well as specific wells, are discussed, illustrating different characteristics, stimulated fracture geometry, and the performance of the completion. Three out of the nine wells in the same pad are examined in more detail. The perforation and plug technique was used for Well F in the south side of the pad while Well B and Well G used the ball and sliding sleeve method. The characteristics of each of these wells are explored, along with how the natural stresses and completion technique affected them.

Geological Background

The area investigated is the Muskwa Shale play in northeastern part of British Columbia. It is bordered by carbonate plays of the Upper Keg River and Slave Point formations. The Muskwa Shale is known to be an organic-rich, silica-based shale and is generally very brittle and displays unique fracture characteristics.

Method

Two different completion techniques were used for this project: - (1) perforation and plug and (2) ball and sliding sleeve. Both methods are common completion techniques used for horizontal wells in unconventional plays. The perforation and plug method (Meehan, 2010) is a stimulation technique that involves running a perforation gun down the well to perforate multiple clusters of shots in each treatment stage. The gun is removed and a mixture of fluids and proppants are pumped into the well to stimulate the rock. Finally, a plug is placed within the well to isolate that stage from the next treatment interval. This is repeated until all the stages are stimulated. A perforation and plug technique was used on the 4 westernmost wells on the pad; C, D, E and F. Twenty stages each were pumped for the C and D wells on the north side and fifteen stages each for the E and F wells on the south side of the pad.

The other completion method is the ball and sliding sleeve. It is an open-hole technique employing multiple mechanically activated sliding sleeve ports and packers placed within targeted sections of the wellbore to provide stage isolation. Different sized balls are dropped when the sleeves open into corresponding sized seats at a target point in the well. Once the balls are properly seated, the flow of fluids is blocked, increasing back pressure causing the sleeve port to open (Maxwell et al., 2012). This method was used for wells 0, B, G, and H: with 0 well completing only eight stages, twenty stages for the B well, and fifteen stages for the G and H wells.

Data

For this project, there are over 29,000 events located in this pad. There is an average total fracture length of >1km for both the north and south side of the pad with a dominant fracture azimuth of 70°. The maximum horizontal stress orientation in this region from the World Stress Map Project (Heidbach et al., 2008) is predominantly 50º-60º (Figure 2). The faults and lineaments maintain a primarily NE-SW orientation with a NW-SE secondary orientation. The majority of the wells show NE-SW linear fracture trends. In general, the microseismicity in the heel stages show a more clustered character than events in the toe. The southern wells show larger amplitude events with higher-event density than the northern wells. There is less microseismicity on the 0 well compared to the rest of the wells.

The b-values for each well were calculated. A b-value is a statistical measure of the relationship between event magnitude and the number of events that occur at that given magnitude or greater. The b-value is based on work by the Gutenberg and Richter (Htwe, and WenBin, 2008), as shown below, where:

$$\mathrm{Log}_{10}N = a - bM$$

M is magnitude.

N is the number of events having a magnitude of M or larger.

Variables *a* and *b* represent intercept and slope, respectively.

In our study, the slope is determined by the linear portion of the data. Departures from the linear trend occur at lower and higher magnitudes due to sensor limitations, aperture limitations, and the infrequency of larger events. The purpose of calculating b-values is to distinguish between the types of stress leading to failure during treatment. Event populations with a b-value around 2 correlate to hydraulically-induced rock failures while values of approximately 1 are associated with natural fault- related events.

Well F (Figure 3), completed using the perforation and plug method, shows well developed linear fractures measuring >1.5km in length for the early stages. This suggests that the NE-SW pre-existing fractures are being intensely reactivated creating long, linear microseismic trends. The plane of the fracture is aligned with the corresponding perforation section: there is little stage-to-stage encroachment. The reactivation of these pre-existing fractures is very evident. The fractures grow across and beyond the four wells in the pad. This same linear trend can be seen for most of the stages except the last five stages which show less energy and linear development as the energy clusters towards the heel. This could suggest that there is a fault in the NW-SE direction, suppressing microseismicity from growing outwards during the stages towards the heel. In this later section of the well, there is also evidence of stage energy propagating back into the earlier stages. The b-value calculated for this well was 2.7,1 suggesting that the fractures are hydraulically-induced rock failures. They follow the dominant fracture azimuth of 70° creating long linear features.

Well B (Figure 4) expresses remarkable characteristics. Stages one through nine show well developed planar fracture lengths symmetrical to the wellbore. The longest fracture length measured in stage 9 is approximately 1.4 km (shown in light purple). The fractures likely follow the natural stresses of the rock. There is evidence in stage 10 of an azimuth change to ~220° suggesting a deformation likely due to a fault structure. There is a completion malfunction after stage 10; all the subsequent energy is concentrated toward the heel of the well. The completion report states that all pumping went according to plan, but the microseismic suggests otherwise. The microseismicity from this well was further investigated, determining two additional dip-slip focal mechanisms present; b-values were calculated by mechanism. The red mechanism in Figure 5, with a b-value (1.67) appears around the stages where the azimuth deviates. This does not conclusively point to a fault-related event but may be interpreted as a pre-existing geological feature which has the potential to be interpreted as a sub-seismic fault.

Well G (Figure 6), completed using the ball and sliding sleeve method, shows well developed, long linear fractures present in the early stages much like Well F. This further suggests that the NE-SW-trending pre-existing fractures are being reactivated to create long, linear features. Later stages show less energy and linear development with energy clustering towards the heel. This could suggest that there is a fault in the NW-SE direction suppressing microseismicity along the NE-SW trend during the stages towards the heel stages. There is also evidence of stage energy propagating back into the early stages. The b-value calculated for well G is 2.23- indicating that the fractures are hydraulically-induced rock failures. The microseismic trends follow the dominant 70° fracture azimuth and create long linear features, in this case growing across all 4 wells. A summary of the F, B and G wells is given in Table 1.

We computed the total fracture surface area, fracture volume, Stimulated Rock Volume (SRV), and the average SRV/stage from the microseismic pointsets. The total fracture surface area is double the sum of fracture length multiplied by fracture height. The total fracture volume is the sum of fracture void space in the volume, calculated from fracture areas and apertures. SRV is the volume of geocellular cubes

that have fracture properties (the affected rock matrix) (Williams-Stroud and Eisner, 2011). When average SRV/stage are compared, the B Well value is lower than for both the F and G wells, likely due to the completions malfunction.

The G well, completed using the ball and sleeve method, has an average SRV/stage of 8,872,941 m^3, while the F well, completed using the perforation and plug method, had an average SRV/stage of 5,345,295 m^3. A comparison of normalized SRV values does not conclusively indicate an advantage of one completion method over the other.

Discussion

The monitoring method used ensures areally unbiased monitoring across all wells, with consistent event location uncertainty. This allows more confidence in the interpretations of the events across the array and supports the idea that variation in microseismicity from well to well are due to local geological heterogeneity in the Muskwa Formation.

The results presented show that long linear fractures are present in the G and F wells, but that these fractures change to a more clustered characteristic towards the heels of these wells. This is possibly due to the presence of a pre-existing fault structure that prevents fracture development by allowing treatment fluids and pressures to leak away, rather than creating microseismic events and fractures as seen in the toe stages. Completion strategies have not contributed to the differences in microseismicity seen on these two wells.

The B well exhibits long linear fractures towards the toe of the well. A sub-seismic geological feature with a different b-value and source-mechanism characteristics is seen around stage ten. There was a completions malfunction that prevented the planned completion of the rest of this wellbore, resulting in lost time, resources, and money.

Conclusions

In this case study we review an example of the natural fractures and faulting characteristics of the Muskwa Shale play in Northeastern British Columbia. The data collected displays distinct growth characteristics and trends across the whole pad. There is a dominant fracture azimuth of 70° which is the general trend the induced fractures follow. Additionally, there is cause for further investigation about different focal mechanisms and b-values to explain these characteristics. The total fracture surface area, fracture volume, Stimulated Rock Volume (SRV), and the average SRV per stage from the microseismic events were also computed for further analysis.

The implications of the microseismic data presented indicate that monitoring of the wells has highlighted the differences in completion response of the Muskwa Formation over small distances across the pad, between wellbores and from stage to stage within the same wells. The data allows comparisons and similarities to be examined, aiding planning of practices and strategies for future drilling and completion in the Muskwa Formation.

Acknowledgements

We would like to give a special thanks to the company that supplied the data and help for making this article possible. We would also like to thank William Barker and Paige Snelling for helping interpret the data.

References Cited

Heidbach, O. Tingay, M, Barth, A., Reinecker, J., Kurfeβ, D., and Müller, B., 2008, World Stress Map: http://dc-app3-14.gfz-potsdam.de; also http://dc-app3-14.gfz-potsdam.de/pub/stress_maps/stress_maps.html (website accessed June 2, 2014).

Htwe, Y.M.M., and S. WenBin, 2008, Gutenberg-Richter recurrence law to seismicity analysis of southern segment of the Sagaing Fault and its associate components: World Academy of Science, Engineering and Technology 50 2009 (http://174.122.150.229/~gripwebo/gripweb/sites/default/files/Gutenberg-Richter%20Recurrence%20Law.pdf) (website accessed June 2, 2014).

Kratz, M., A. Aulia, and A. Hill, 2012, Identifying fault activation in shale reservoirs using microseismic monitoring during hydraulic stimulation: Source mechanisms, b values, and energy Release rates: http://www.cseg.ca/publications/recorder/2012/06jun/Jun2012-Identifying_Fault_Activation_in_Shale.pdf.

Maxwell, S., Chen, et al., 2012, Microseismic monitoring of ball drops during a sliding sleeve frac: http://www.cspg.org/documents/Conventions/Archives/Annual/2012/085_GC2012_Microseismic_Monitoring_of_Ball_Drops.pdf (website accessed June 2, 2014).

McPhail, S., W. Walsh, and C. Lee, 2008, Shale units of the Horn River Formation, Horn River Basin and Cordova Embayment Northeastern British Columbia: http://www.empr.gov.bc.ca/Mining/Geoscience/PublicationsCatalogue/OilGas/OpenFiles/Documents/PetroleumGeology/PGOF2008-1.pdf (website accessed June 2, 2014).

Meehan, D.N., 2010, Completion techniques in shale reservoirs: http://blogs.bakerhughes.com/reservoir/2010/09/18/completion-techniques-in-shale-reservoirs (website accessed June 2, 2014).

The Cordova Embayment, 2012, http://northof56.com/oil-gas/article/the-cordova-embayment (website accessed June 2, 2014).

Williams-Stroud, S.C., and L. Eisner, 2011: Stimulated fractured reservoir DFN models calibrated with microseismic source mechanisms: ARMA 10-520, 8p.

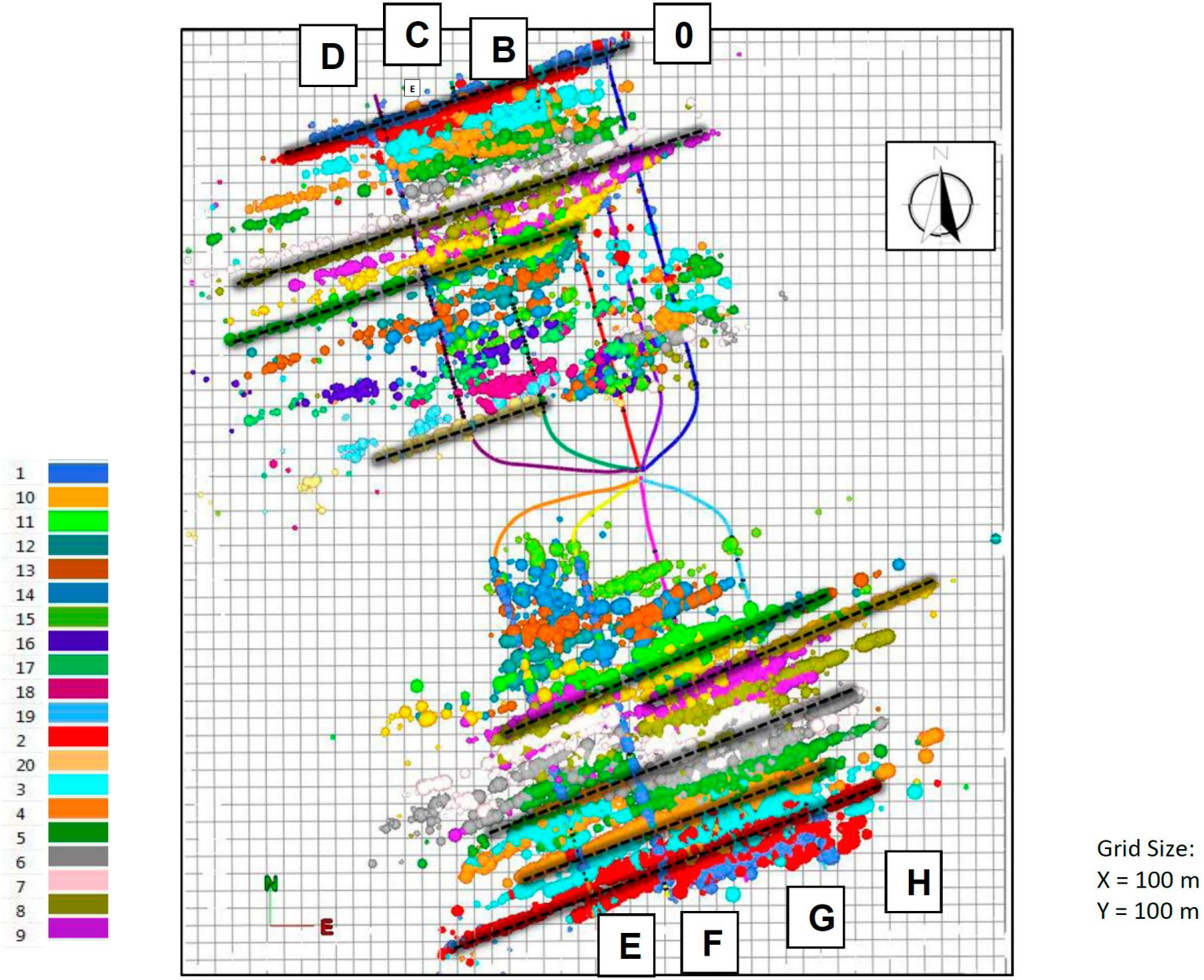

Figure 1. Well field map depicting the well layout and the microseismic events, sized by energy and colored by stage. Microseismic event trends are shown as dashed lines.

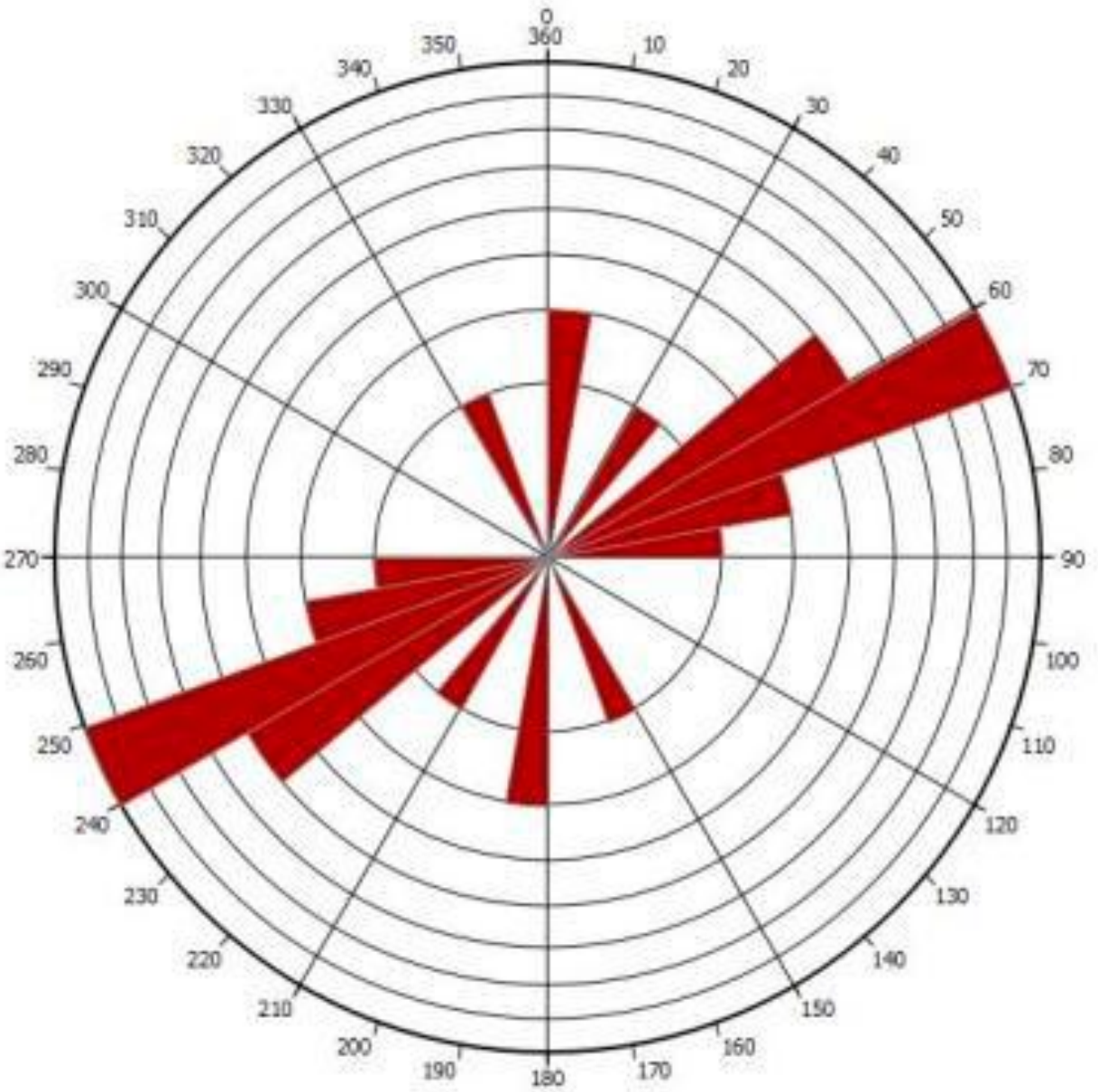

Figure 2. S_{Hmax} from World Stress Map Project of the area, showing a predominantly 50º-60º horizontal stress orientation.

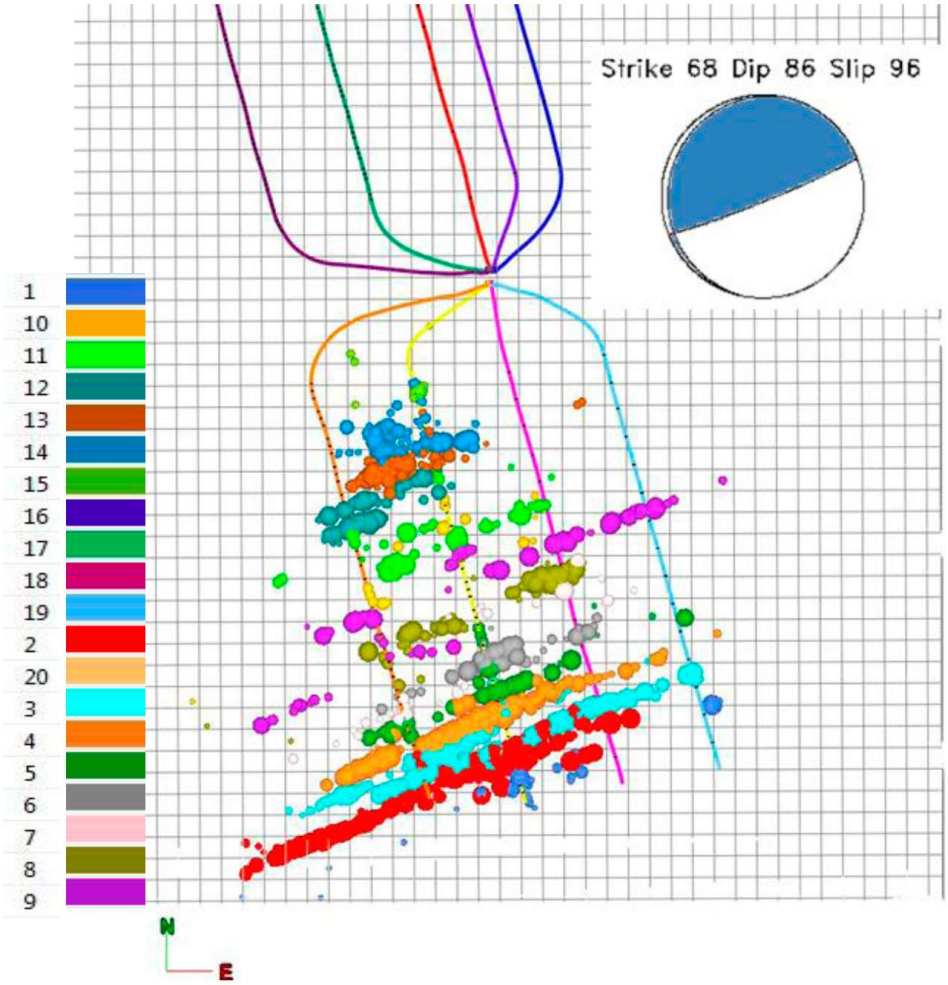

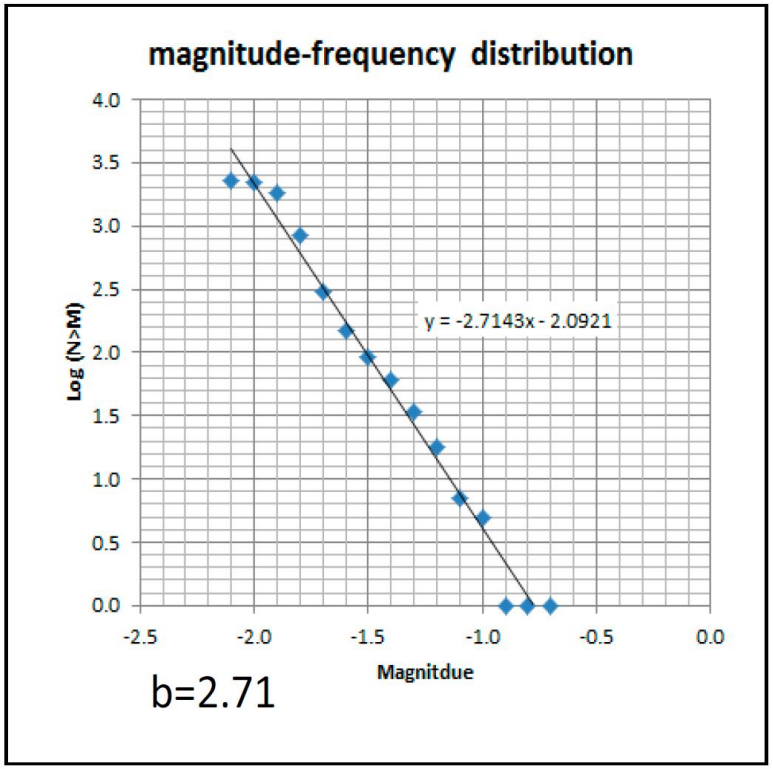

Figure 3. (left) Well F, perforation and plug completion map view; events are sized by energy and colored by stage. (right) b-value analysis for Well F events.

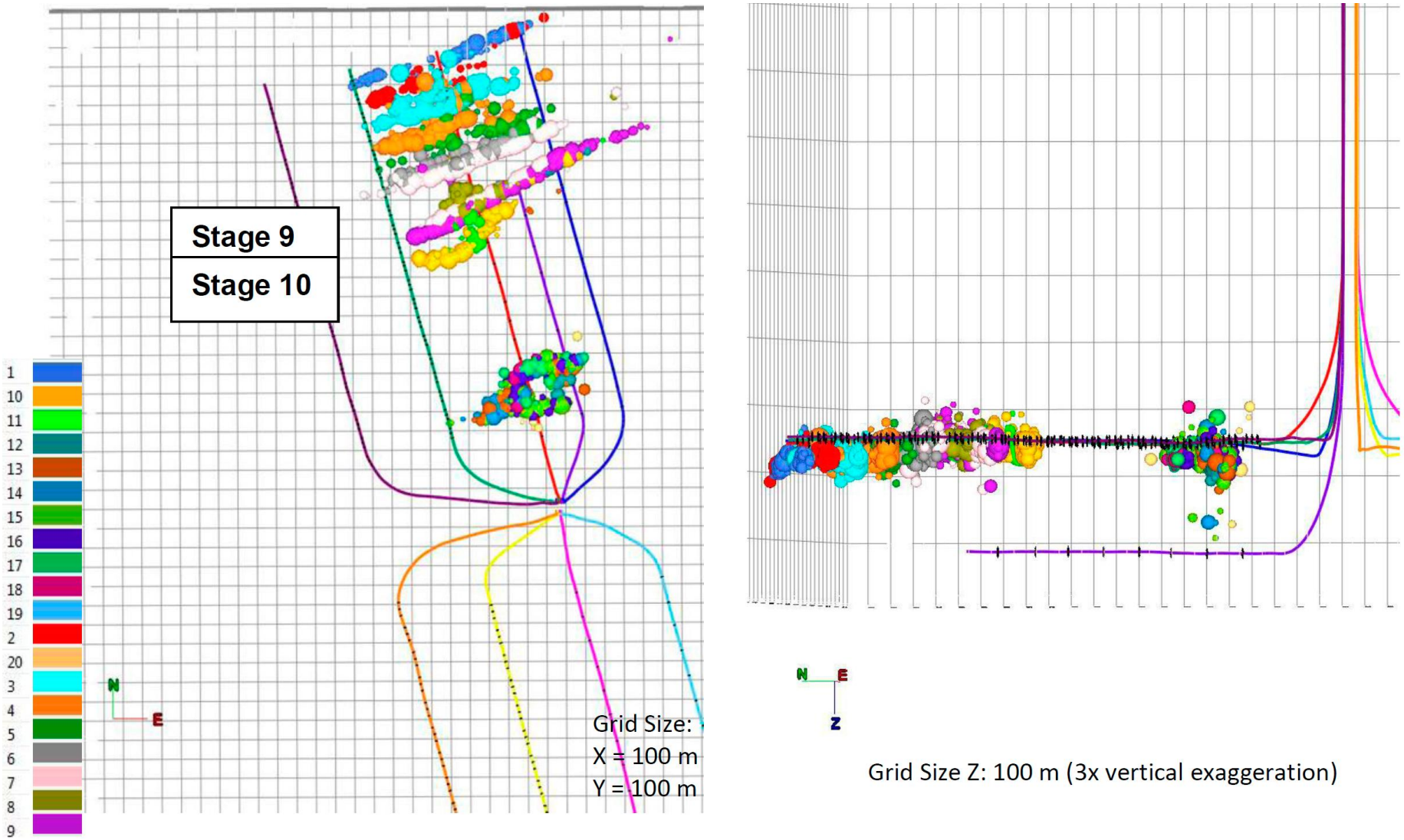

Figure 4. Map and depth views of Well B. Microseismic events are sized by energy and colored by stage.

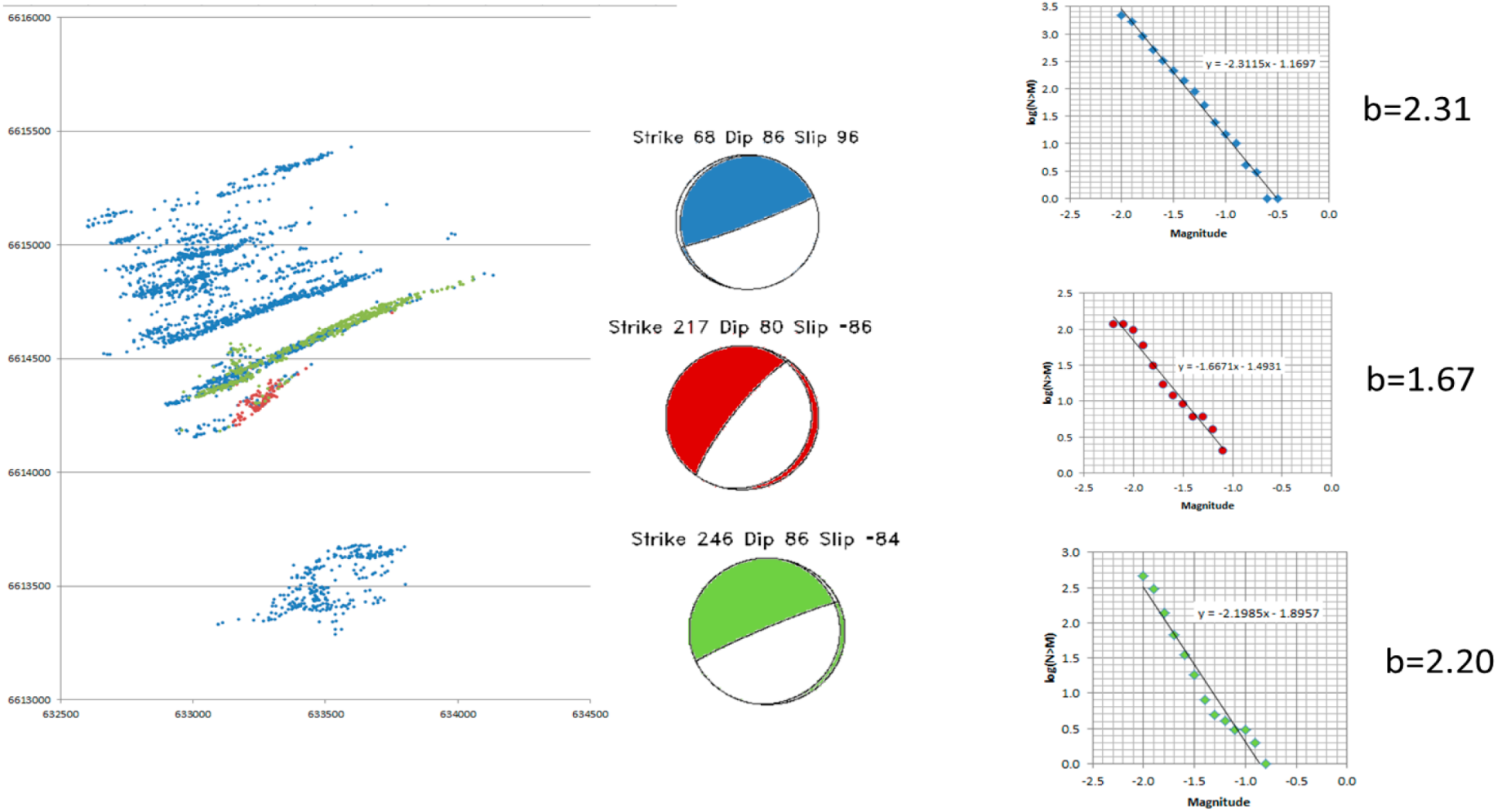

Figure 5. Microseismic events from Well B colored by mechanism. Corresponding b-value calculations are shown.

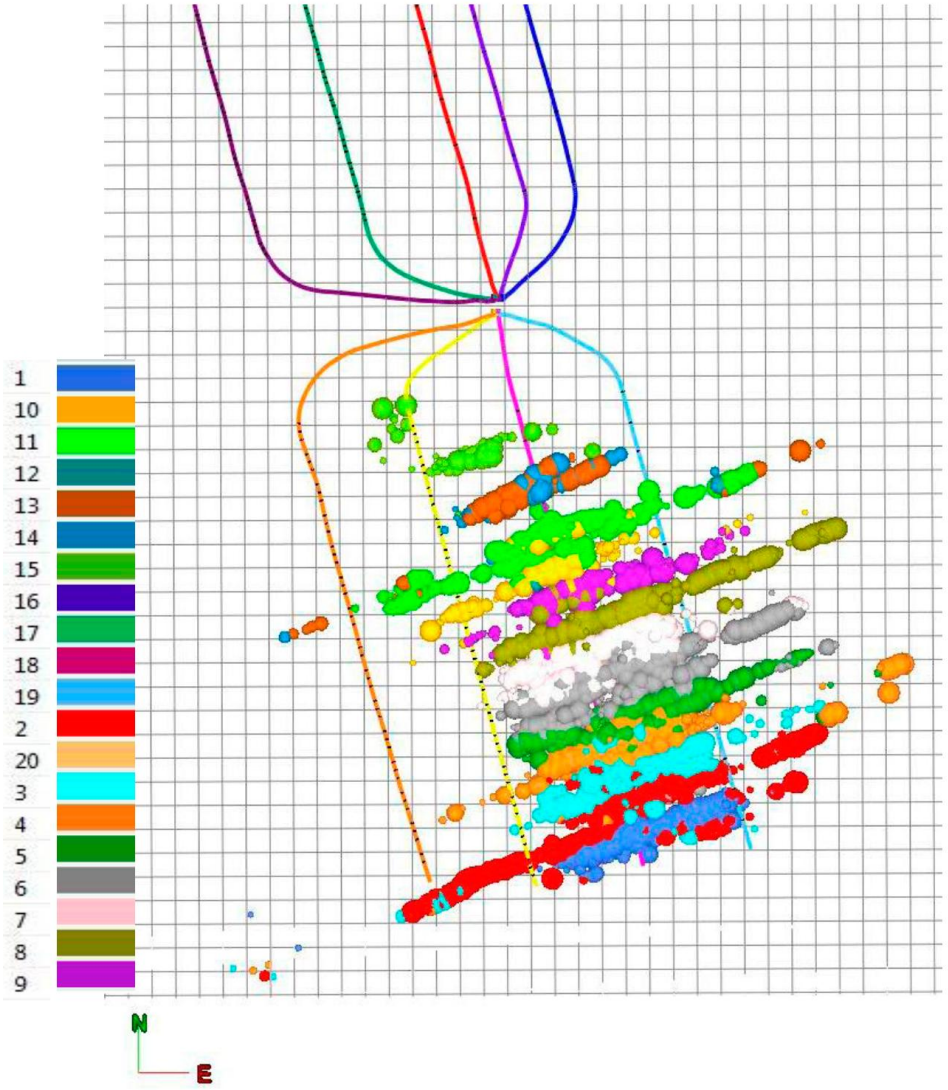

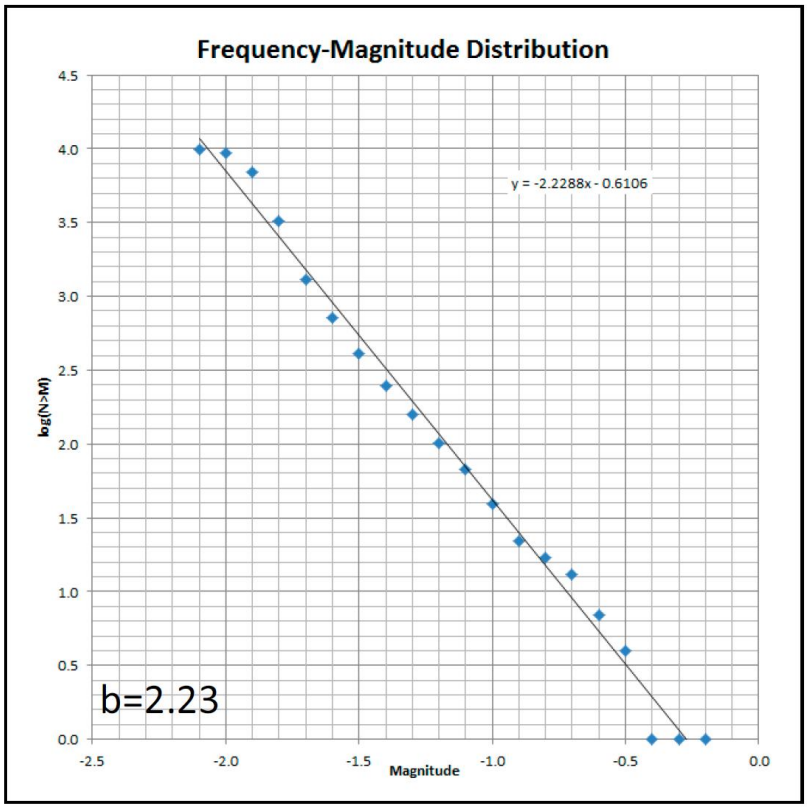

Figure 6. (left) Well G, ball and sliding sleeve completions in map view, showing microseismic events sized by energy and colored by stage. (right) b-value analysis for Well G events.

Well	F	B	G
Total Fracture Surface Area (m^2)	4,190,900	4,146,200	17,931,900
Total Fracture Volume (m^3)	9,263	9,056	39,277
Stimulated Rock Volume (m^3)	80,179,412	53,629,412	133,094,118
Average SRV/stage (m^3)	5,345,294	2,681,471	8,872,941

Table 1. Total fracture surface area, fracture volume, SRV, and normalized average SRV for Wells F, B and G.